STEEP, SHORT-CRESTED WAVES AND RELATED PHENOMENA

A. R. Kolaini

National Center for Physical Acoustics
University of Mississippi
Coliseum Drive
Oxford, MS 38677 USA

Abstract Steep, short-crested waves, as well as a large variety of three-dimensional propagating wave patterns have been created in laboratory, utilizing a plunging half-cone. Monochromatic waves, over a range of frequencies and amplitudes through breaking and including soliton wave groups near resonance, have been observed and studied in a small wave flume. This monochromatic wavemarker creates complex wave patterns which depend upon the wavemaker shape, its frequency, and the tank width. The theory is presented along with computer simulation and experimental data to describe these three-dimensional waves. The effect of viscosity at the wall is taken into account to explain the attenuation of wave energy down-tank. In the neighborhood of the first cut-off frequency, strong nonlinear-effects were observed. Symmetric-standing sloshing waves generated at the wavemaker spontaneously form a moving hump (soliton), which propagates very slowly down-tank. The hump then builds up again in time at the wavemaker and the process is repeated. In the case of two-mode propagation, waves produced are diamond-shaped patterns and propagate in such a way that the amplitude of individual wave crests oscillate with distance down-tank. As a result, intermittent breaking can be caused to occur at specific locations away from the wavemaker. The inception of breaking was found to occur over a range of wave steepness, from a minimum (consistent with other experiments, and decreasing with short-crestedness) to a maximum (close to the Stokes limiting steepness). Breaking was observed to occur, providing: (i) the wave steepness exceeds a threshold (minimum) value; and, simultaneously, (ii) the propagating wave crest reaches a maximum and begins to decline. These observations suggest a new criteria for the inception of breaking.

Key Words Wave Propagation, Steep Waves Propagation, Steep Short Crested Waves

چکیده امواج عمیق با دامنهٔ کوتاه همراه با اشکال متنوع دیگری از امواج سه بعدی توسط تولید کنندهٔ موج half-coneدر آزمایشگاه ایجاد شده است. امواج تک رنگ برای محدوده ای از فرکانسها و دامنه از طریق breakingکه شامل امواج گروه Solitonدر نزدیکی تشدید میشود، مورد مطالعه قرار گرفته است. ایجاد کنندهٔ امواج تک رنگ، امواج پیچیده ای ازنظر شکل ایجاد میکند که بستگی به شکل، فرکانس و پهنای مخزن دارد. تئوری مربوط همراه با شبیه سازی کامپیوتری و نتایج مربوط به آزمایشهای عملی برای تشریح این امواج سه بعدی ارائه شده است. تأثیر غلظت در دیواره برای ایجاد میرائی انرژی موج در داخل مخزن درنظر گرفته شده است. در همسایگی اولین فرکانس قطع اثرات غیر خطی شدیدی ملاحظه شده است. امواج متقارن ساکن که توسط تولید کننده امواج ایجاد میشود، برآمدگی متحرکی ایجاد میکند که به آرامی در امتداد مخزن منتشر میشود. این برآمدگی سپس مجدداً توسط ایجاد کنندهٔ موج تولید میشود واین فرایند تکرار میشود. درمورد انتشار امواج با دو مد، امواج تولید شده، الماسی شکل بوده و طوری انتشار می یابد که دامنهٔ قلهٔ هریک از امواج درطول مخزن نوسان میکند. نتیجتاً توقف موج در نقاط مختلف مسیر درطول پخش میتوان ایجاد کرد. مشاهده شده است که توقف موج برای عمق های مختلف از یک حداقل تا یک حداکثر اتفاق می افتد مشروط برآنکه: عمق موج ازحد مشخصی بیشتر باشد و همزمان با آن قلهٔ موج پخش شونده ازیک ماکزیمم گذشته باشد و شروع به کم شدن کرده باشد. مشاهدات مذکور برای معیارهای توقف موج، پیشنهاد جدیدی را مطرح مینماید.

INTRODUCTION

Steep waves at sea are short-crested and it is highly desirable to produce such waves in a laboratory tanks for the purpose of testing the response of platforms and ships, as well as to study nonlinear effects such as breaking wave loadings on platforms and nonlinear sloshing waves in the form of solitons. At present,

waves are produced in a water basin using segmented programmable plunging or paddle type wavemakers [1-4]. Steep short-crested waves can be produced in a laboratory tank by utilizing a simple three-dimensional wavemaker [5,6]. These non-planar wavemakers can produced complex linear and nonlinear gravity waves.

The existence of discrete standing wave modes in a closed tank is well known [7] and was first studied by Ursell [8] by producing edge waves on sloping beach. The most extensive experimental work on sloshing waves is reported by Bornand and prichaid [9] where they produced asymmetric propagating waves by a flat plate oscillating about a central vertical hinge close to the first cut-off frequency. More recently, experimental and theoretical studies of nonlinear effects over a range of cut-off frequencies have been reported [10-12]. These works emphasize asymmetric waves produced by paddle-like wavemakers and may be regarded as complementary to our own work, which emphasizes symmetric waves produced by plunging conical shape, and has been particularly motivated by an interest in the practical application of such a wavemaker. A steady non-propagating soliton-like solution was observed experimentally by Wu et al. [13]. An analysis of this soliton was made by Larraza and Patterman [14] by employing the nonlinear Schrödinger equation.

The phenomena of breaking waves is one of the fundamental, but unsolved problems in hydrodynamics [15]. The statistics of the steeper and most energetic waves is of great importance for ocean engineering [16] and is very much determined by breaking. Moreover, the impact of breaking waves against ships and offshore structures may cause serious safety problems and structural damage to systems [17].

We have carried out theortical and experimental studies of monochromatic waves produced by plunging semi-cone. This study introduces a new wavemaker which produces three-dimensional waves with varying heights along each crest in a narrow tank. Understanding short-crested waves is not only important on generating stochastic random waves, it may also serve as a basis for the investigation of three-dimensional breaking waves and their effect on offshore structures, nonlinear sloshing waves, and experiments which will improve the understanding of radar scattering in a laboratory tank.

THEORY

Consider the propagation of small amplitude surface gravity waves in a semi-infinite deep channel of width **b**, where waves are being produced by an oscillating arbitrary shaped wavemaker mounted at one end of the channel. Assuming irrotational motion, incompressible fluid, the problem of predicting the wave patterns generated by a periodically moving wave generator can be described in terms of a potential function, ϕ, and free surface elevation, ζ. A dispersion relationship can be derived by using the classical linearized boundary conditions,

$$\overline{\lambda_n^2} = \frac{1.0}{\left[\overline{\omega^4} - n^2\right]} \quad , \qquad (1)$$

with $\overline{\lambda_n} = \frac{\lambda_n}{b}$, and $\overline{\omega^2} = \frac{b\,\omega^2}{2\pi g}$ where λ_n is the wavelength, g is the gravity, n is an integer, and ω is the frequency of the oscillation. These derivations are valid for deep water where $k_0 h < \frac{\pi}{2}$ with $k_0 = \omega^2/g$ and h is the water depth. A plot of the dispersion relationship is given in Figure 1. This Figure reveals the generation of linear propagating waves away from cut-off frequencies. At cut-off frequencies, linear theory predicts infinite wavelengths with zero group velocities, while experimental observation has suggested finite wavelengths. Consequently, linear theory is not an

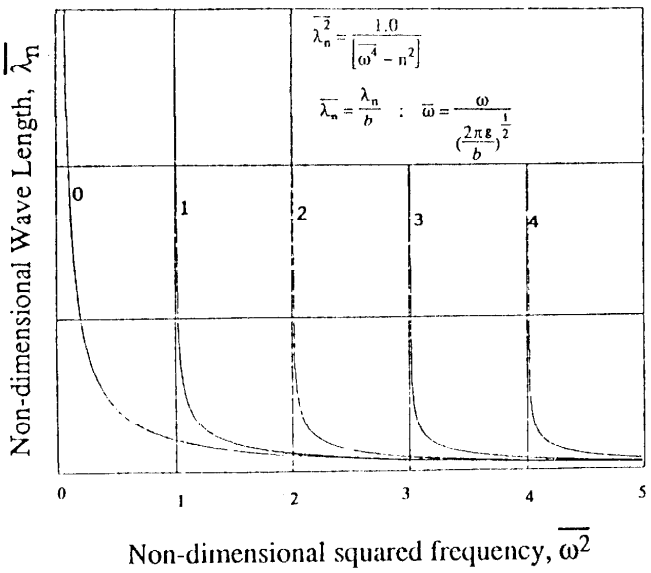

Figure 1. Dispersion waves for symmetric modes in a channel of width b.

adequate predictor at these discrete frequencies. Below a linear theory is given for the concial wavemaker which generates propagating waves away from cut-off frequencies. At the neighborhood of the first cut-off frequency, occurrence of soliton waves were observed. Experimental observation of these nonlinear waves is given with the comparison to the existing theory.

Conical Wavemaker Model

Havelock [18] examined the three-dimensional periodic oscillating source of strength, $qe^{i\omega t}$, located at the depth of f, beneath the free surface. In a corrdinate with the origin O taken to be the undisturbed water surface, with a positive depth z, projected vertically downward, he assumed the classical wave theory of irrotational, incompressible, fricitionless, and no surface tension for the wave field. For a periodic motion of frequency ω, using the linearized free surface boundary conditions, he gave the following expression for the potential function:

$$\phi(r', z; k_0) = 2\pi k_0 q\left(\frac{2}{\pi k_0 r'}\right)^{\frac{1}{2}} \sin(\omega t - k_0 r' + \frac{1}{4}\pi)\, e^{-k_0(f+z)} \qquad (2)$$

where r' is the radial distance and f is the location of the source. Equation 2 is an asymptotic solution to the equation for a source with strength q, in an infinite fluid domain. This periodic source oscillation is then restricted to oscillate in a fluid domain bounded by tank's walls. The summary of the derivation of methods used to model a conical wavemaker with the aforementioned results is given below.

Using method of images whereby the source, symmetrically placed between walls, is replaced by its equivalent, an infinite number of identical cascade sources are displaced along the plane, x = 0, with spacing b (Figure 2). The potential function for these identical sources is

$$\phi_n(x,y,z) = 2\pi q \sum_{-\infty}^{\infty} \left[\frac{2}{\pi k_0 \sqrt{x^2 + (y + 2n\pi b)^2}}\right]^{\frac{1}{2}} k_0 \sin(\omega t - k_0 \sqrt{x^2 + (y + 2n\pi b)^2} + \frac{\pi}{4})\, e^{-k_0(f+z)}. \qquad (3)$$

Equation 3 is transformed into the Fourier integral equation by locating an infinitesimal source at a distance y' from the origin and distributing source strength along the y axis

$$\phi(x,y,z,t) = -2\pi i\, q(f)\, e^{-k_0(f+z)} \int_{-\infty}^{\infty} k_0 \left(\frac{2}{\pi k_0 r'}\right)^{\frac{1}{2}} \times e^{i(\omega t - k_0 r' + \frac{\pi}{4})} a(y')\, dy', \qquad (4)$$

where $r' = \sqrt{x^2 + (y - y')^2}$ and $\tilde{a}(\kappa) = \int_{-\infty}^{\infty} a(y')\, e^{-i\kappa y'} dy'$. The $\tilde{a}(k)$ is the Fourier transform of a(y'). Assuming a periodic delta function for $\tilde{a}(k)$ located at $k = k_n = \frac{2\pi n}{b}$ and substituting it in Equation 4, an expression for the potential function is derived where source strength is also distributed along the z axis.

$$\phi_n(x,y,z,t;\omega) \cong -i \int_0^f q(f')\, e^{-k_0(Z+f')}\, df' \int_{-\infty}^{\infty} k_0 \left(\frac{2}{\pi k_0 r'}\right)^{\frac{1}{2}} \times e^{i\left(\omega t - k_0 r' + \kappa_n y' + \frac{\pi}{4}\right)} dy' \qquad (5)$$

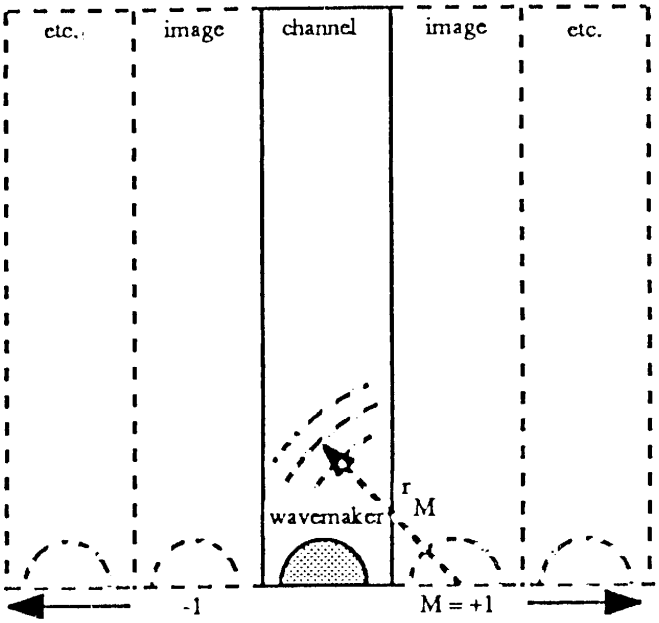

Figure 2. A schematic illustration of conical wavemaker and tank walls. The tank walls are replaced by an infinite number of images of the wavemaker.

In Equation 5, the phase function $\psi(y') = \omega t - k_0 r' + k_n y' \mp \pi/4$. As y' approaches infinity, the second integral in Equation 5 takes an asymptotic form which is determined entirely in terms of the point at which the phase function $\psi(y')$ is stationary; i.e., at a value of $y' = y'_0$, $\frac{\partial \psi}{\partial y'} = 0$. The criterion for this method which is called Kelvin's Stationary Phase Method for variables r'_0 and y'_0 are

$$y'_0 = y + \frac{x\kappa_n}{(k_0^2 - \kappa_n^2)^{\frac{1}{2}}} \quad \text{and} \quad r'_0 = \frac{x k_0}{(k_0^2 - \kappa_n^2)^{\frac{1}{2}}}. \tag{6}$$

Expanding $\psi(y')$ in a Taylor series about $y'=y'_0$, and applying the condition $\frac{\partial \psi}{\partial y'} = 0$ with the assumption that $\psi(y')$ is a slowly varying function relative to $e^{i\psi(y')}$ allows the condition $\psi(y') \approx \psi(y'_0)$ to be used; y' is near y'_0, i.e., $|y' - y'_0| \leq 0$. The first integral in Equation 5 can be solved by using the conical form of the wavemaker and distributing the source strength along the **z** axis in such a way that the conical shape with 38 degrees angle is preserved. On the surface of the cone, the following condition is applied,

$$\vec{V} \cdot \vec{n} = 0 \quad \text{or} \quad (U + u) n_z + v_r n_r = 0, \tag{7}$$

where $\vec{V}$ is the fluid velocity on the wavemaker, u and r_r are the perturbation velocities and U is the free stream velocity. By assuming U>>u, and applying slender body approximation, the source strength at a location f' along the **z** axis can be derived,

$$q(f') = \pi (f - f') \frac{s\omega}{2f} \delta, \tag{8}$$

where δ is the cone angle and is related to the height f and radius R of the cone. Upon introducing these approximations and integrating Equation 5, a relation for potential function can be obtained,

$$\phi_n(x,y,z,t) \cong \sum_{n=0}^{\infty} (\frac{\pi}{2})^{\frac{1}{2}} s\omega \frac{(\frac{R}{f})(f k_0 + e^{-k_0 f} - 1)}{f k_0 \sqrt{k_0^2 - \kappa_n^2}} e^{i(\omega t - x\sqrt{k_0^2 - \kappa_n^2})} \times e^{-k_0 z} \cos(\kappa_n y). \tag{9}$$

Using the linearized free surface profile

$$\zeta = \frac{1}{g} \frac{\partial \phi}{\partial t} \quad \text{at} \quad z = 0, \tag{10}$$

the free surface profile can be derived

$$\zeta(x,y,t;\omega) = \mathrm{Re} \sum_{n=0,1,2,\ldots}^{\infty} -i (\frac{\pi}{2})^{\frac{1}{2}} s (\frac{R}{f}) \frac{(f k_0 + e^{-k_0 f} - 1)}{f \sqrt{k_0^2 - \kappa_n^2}} \times e^{i(\omega t - x\sqrt{k_0^2 - \kappa_n^2})} \cos(\frac{2n\pi}{b}). \tag{11}$$

From the dispersion relation (Equation 1, Figure 1), it is evident that for each frequency, the number of waves is determined by the number of propagating modes. The resulting patterns, the sum of a discrete number of waves of different wave lengths, will produce irregular waves. For frequencies below the first cut-off (i.e. $f < 1.31$ Hz), there is only one propagating mode, n=0. Excitation of the wavemaker with frequencies between the first and second cut-offs (i.e.

1.51 Hz < f < 1.85 Hz) results in two propagating modes, n=0 and n=1. The wave patterns for the first and second modes can be written in terms of an irregular wave with a modulating beat

$$\zeta(x,0,t;\omega) = \left[(A_0^2 + A_1^2) + 2A_0A_1\cos(k_0 - k_1)x\right]^{\frac{1}{2}} \times \cos\left[\left(\frac{k_0+k_1}{2}\right)x + \tan^{-1}\beta(x) - \omega t + \frac{\pi}{2}\right] \quad (12)$$

where $\beta(x) = \frac{A_0 - A_1}{A_0 + A_1}\tan\left[\left(\frac{k_0 - k_1}{2}\right)x\right]$ and $k_1 = \sqrt{k_0 - \kappa_1}$, with A_0 and A_1 being coefficients in Equation 11. At the first cut-off frequency $k_1 \rightarrow 0$, as a result $\beta(x) \rightarrow -\tan\left(\frac{k_0}{2}x\right)$, and consequently, irregular wave disappears. This proves that no wave propagates at the first cut-off frequency. The irregularities also disappear for these wave patterns only in the case where $A_0 = A_1$. By adding more modes to the wave, patterns themselves become increasingly complex and the algebra is more tedious to carry out.

Sinusoidal gravity waves generally suffer attenuation as a result of loss of energy due to viscous effects. The energy dissipation due to the side walls are enhanced by the three-dimensionality of waves because their group velocity is slower than planar waves (Figure 1). With the assumption of deep water waves the attenuation of the waves due to the bottom wall is neglected. Ursell (1952) studied the viscosity effect for waves on a sloping beach. He considered single mode, non-planar propagating waves for deep water and gave an estimated value for the attenuation coefficient which is valid for frequencies away from cut-offs. While Ursell found the attenuation coefficient for a single propagating wave, this study adapted his analogy by extrapolating it to more than one propagating wave. In a fluid with a low viscosity, the approximated fluid velocity is given by

$$\vec{U} = (U, V, W) = e^{-K'x}\,\text{grad}\,\phi\ , \quad (13)$$

where K' is the attenuation coefficient. The effect of viscosity is to cause a slow attenuation of the waves as they move away from the source of energy. An estimate of the variable K' for waves between the first and second cut-off frequencies is [19],

$$K' = \frac{\kappa_1 k_0}{2\pi^2}\sqrt{\frac{\nu}{2\omega}}\,\frac{\left[5\left(\frac{k_1}{k_0}\right)^2 + 2\left(\frac{k_1}{k_0}\right) + 1\right]}{\left[\left(\frac{k_1}{k_0}\right)^2 + \frac{1}{2}\left(\frac{k_1}{k_0}\right)\right]} \quad (14)$$

where ν is the kinematic viscosity. Equation 14 is valid when the flow field is dominated by the potential function. This expression is not valid when the wavemaker is operated at frequencies close to cut-offs, where the nonlinearity plays an important role.

Nonlinear Sloshing Waves Near the First Cut-off Frequency

Sloshing waves are found in systems where a cut-off frequency has been attained. For example, they can be found in a tank with a wavemaker that generates a typical wavelength λ, and operates at a frequency close to the first cut-off frequency (i.e., $\omega^2 = \frac{2\pi g}{b}$). Waves produced at cut-off frequencies are usually referred to as "sloshing waves" [12,20]. Operating the concial wavemaker near the first cut-off frequency, periodic sloshing waves were observed and hump-shaped waves were formed down-length of the tank. The maximum of these wave height distributions slowly propagates down stream and away from the wavemaker. These waves are categorized as being solition waves.

The most extensive work on nonlinear sloshing waves are reported by Aranha et al. [20] where they derive a third-order nonlinear Schrödinger equation for the propagation of an acoustic wave in a duct generated by wavemaking-like source. Few years later Kit, et al. [12] adapted their theory to gravity waves which are produced in a laboratory tank by using modular wavemaker and generating the first and second modes of sloshing waves. Kit, et al. modified the nonlinear

Schrödinger equation by including the viscosity effect at the wavemaker which results in a propagating soliton waves. Operating the conical wavemaker at the first cut-off frequency produces periodic propagating solitons. The theory given by Kit, et al. was adapted to the conical shape and was reported by Kolaini [19].

EXPERIMENTAL PROCEDURES

Figure 3 shows the photograph of the experimental tank used to generate three-dimensional waves. The wave tank has interior dimensions of 0.9 m × 0.9 m × 21 m (width × height × length). The bottom is covered with a black rubber coating and walls comprise of three quarter-inch thick clear glasses. The wavemaker was stationed at one end of the tank, while at the other end a beach was situated. A vertical wall was mounted to a variable speed motor and was guided between a set of I-beam rails and Teflon bushings. A two-inch gap existed between this wall and a frame which the plate was mounted on. There was also a half-inch gap between the plate and the tank walls. A false wall was placed between the frame and the vertical wall to minimize leakage from the walls and the bottom of the tank. A half-cone wavemaker with an angle of 38 degrees was mounted to the vertical wall with a mean position of 74 cm from the bottom of the tank. The wave heights were measured with capacitance type wave gauges placed in the middle of the tank at small intervals were measured with capacitance type wave gauges placed in the middle of the tank at small intervals along the length of the tank. Before running a set of experiments, the tank was filled with room temperature tap water to a mean depth of 66 cm. Waves were generated by driving the wavemaker sinusoidally, with amplitudes ranging from 2.54 cm to 11.43 cm and frequencies between 0.5 Hz to 2.5 Hz. Wave heights were measured at the middle of the tank in locations 4.2 m to 13 m from the wavemaker. Here we only report measurements of three-dimensional waves between the first and second cut-off frequencies and near the first cut-off frequency.

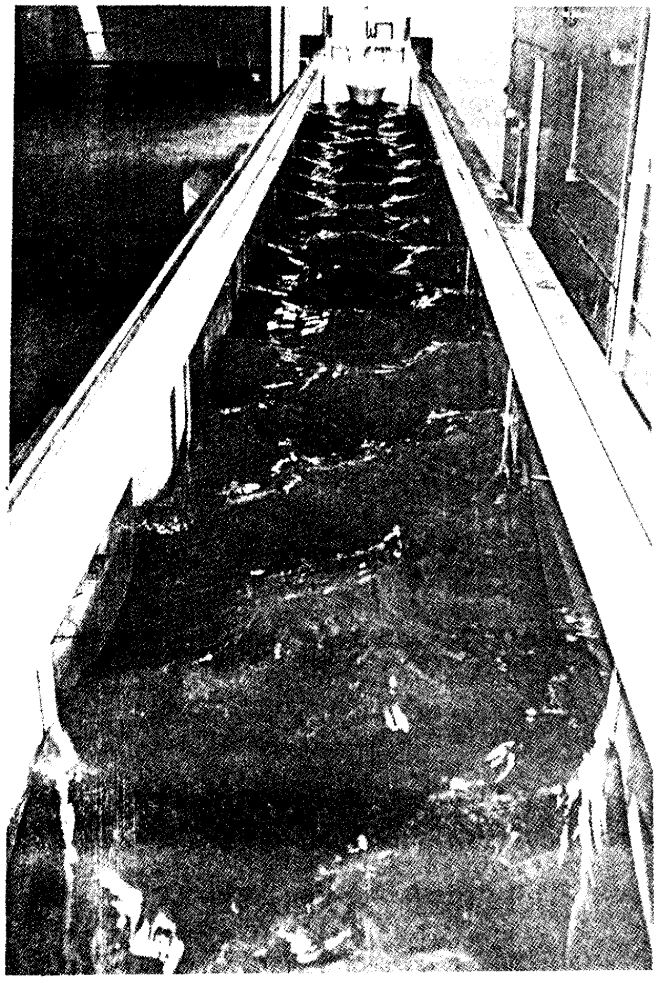

Figure 3. Photograph of wave pattern at the frequency of $f = 1.5$ Hz.

Sloshing waves resulted from operating the wavemaker closer to the first cut-off frequency (i.e., $f = 1.308$ Hz); this frequency was measured using HP 5316B universal counter and was approached from below the cut-off and care was taken to fine tune the adjustment to avoid combining the propagating planar and non-planar waves. The instantaneous surface elevation of the induced wave field was measured with three wave gauges which were located along the center line of the tank and 3 m from each other. Three gauges were also situated across the tank-one along the center line and two closer to the tank walls-within equal distance from the first gauge for the purpose of confirming the symmetricity of the sloshing mode. The outputs of all gauges were sampled simultaneously

with 1000 samples/sec using the Keithly Data Acquisition system and were recorded on magnetic tape for future analysis.

Typical wave traces for three-dimensional waves for frequencies between the first and second cut-off are shown in Figure 4 for wavemaker frequency of f = 1.53 Hz with a wavemaker stroke of 8.4 cm at locations of 4.5 m, 6.10m, 4.6m, 8.8m, and 11m from the wavemaker. The wave heights in all of these figures are normalized with respect to the wavemaker stroke. Differences in the maximum and minimum of these points were averaged to yield average wave heights at several locations along the tank. Located 3m, 6m, and 9m from the wavemaker, the three wave gauge probes measured the amplitudes of the soliton and are shown in Figure 5 for the wavemaker stroke of s = 6.35 cm. This figure shows stable and semi-periodic solitons with small amplitude modulation. For different forcing functions, the speed of the soliton was determined by measuring the distance between probes and recording the time for a soliton to travel from one point to the other. Results of these measured quantities are discussed later.

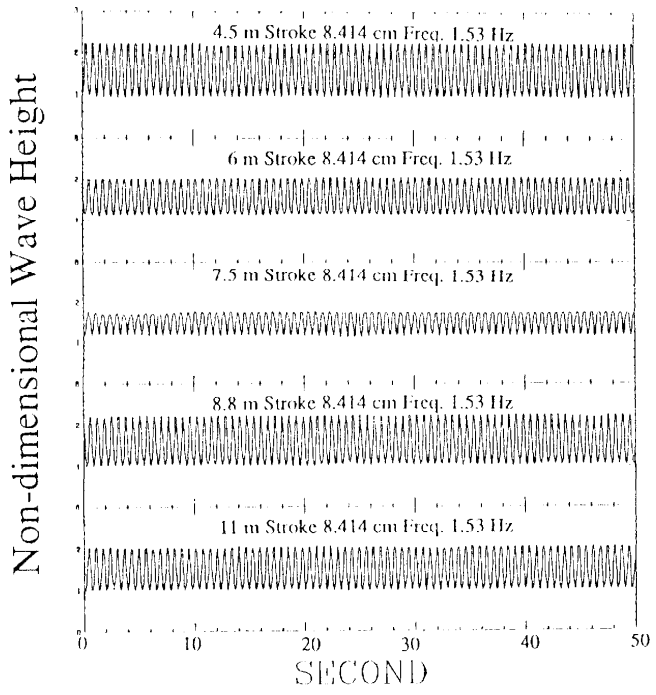

Figure 4. Wave traces for frequency of oscillation of 1.53 Hz, between the first and second cut-off frequencies, with a wavemaker stroke of 8.4 cm at various locations along the tank.

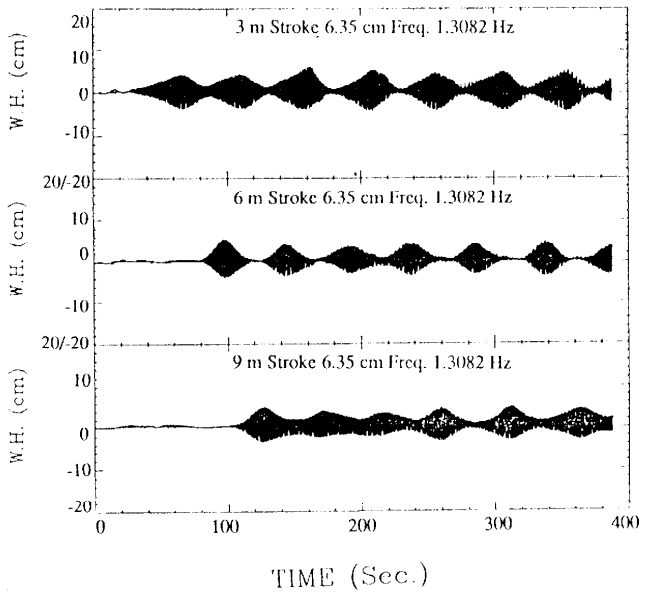

Figure 5. Sloshing wave heights as a function of time at various locations along the channel with wavemaker stroke of 6.35 cm.

Short-crested wavers at moderately high wavemaker strokes become very steep and unstable and ultimately break throughout the tank. Experimental observations of these unsteady, three-dimensional breaking waves were studied. The surface profile measurements for breaking waves were carried out photographically using a movie camera and a light-slit generator consisting of seven 500 watt flood lights placed in series with each other. The 1.5m long generator projected a 2.54 cm thick vertical sheet of light parallel to the sidewalls of the tank. In addition to the generator, a 1.5m long sprayer continuously introduced a fine vapor of rhodamine fluorescent dye onto the water surface. The camera film recorded a glowing line on the water surface which produced an image of the surface profile on Kodak 4-X black and white reversal film. A frame analyzer was used to observed and measure the variation of the wave height prior to, during, and after breaking, and the development, growth, and collapse of the breaker. An AT & T Targa M8 image capture board and Image Pro software was used to measure the

geometry of the evolution of the breaking region.

RESULTS AND DISCUSSION

In section 2 the theory for waves produced by plunging a half-cone was given. A comparison between the measured wave height modulation with respect to distance from the wavemaker and the theory was also given. Since these propagating waves are steep and short-crested, higher wavemaker amplitudes cause these waves to become unstable and break. It is evident from the dispersion relation (Equation 1) that as each cut-off frequency is exceeded, a new propagating mode contributes to the far field wave pattern, resulting in more complex patterns. Thus in applying this equation, waves for each mode are summed with the number of term ***n***. Results of the computer simulation of Equation 11 show the appearance of an appropriate new mode each time a cut-off frequency is exceeded. At a frequency between the first two cut-offs a diamond-like wave pattern results from the superposition of three propagating waves, one wave along the length of the wave tank and the two symmetric ones at an angle of $\theta_1 = \sin^{-1}(\frac{1}{\omega^2})$ with the first wave (Figure 6). A photograph of the wave pattern produced at the frequency of $\bar{\omega} = 1.148$ ($f = 1.5$ Hz) is shown in Figure 3. The equivalent of the sum of the wave patterns are given in terms of an irregular wave

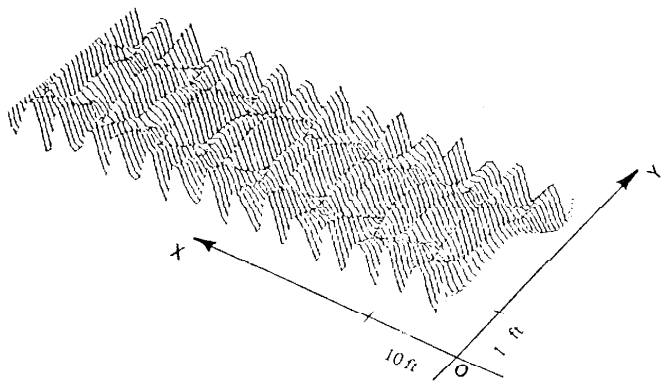

Figure 6. Computer simulation of a wave pattern by half-cone wavemaker ($f = 1.5$ Hz).

with a modulating beat which was characterized in section 2. In Figure 7 the experimental data are best fitted with a square of the modulation curve and are compared with the theoretical beat equation. The experimental results for the local wave height show a decay of the wave height down the channel. This decay was adjusted by estimating the viscosity attenuation coefficient given by Equation 14. An equation for the square of the local wave height modulation which includes the dissipation coefficient is given by

$$H^2 = \left[A_0^2 + A_1^2 + 2A_0A_1 \cos((k_0 - k_1)x - \alpha)\right] e^{-2K'x} \qquad (15)$$

where A_0, A_1, k_0, k_1, and K' were introduced in section 2. An empirically determined small phase contant, α, is added to both the experimental data and the theoretical beat function. However, at higher wavemaker strokes (i.e. s= 11.43 cm), the measured wave height is about 27 percent smaller than the theoretical one. In this case, the lengths of the two basic waves for a frequency of $f = 1.53$ Hz are: $\lambda_0 = 67$ cm and $\lambda_1 = 98$ cm. The

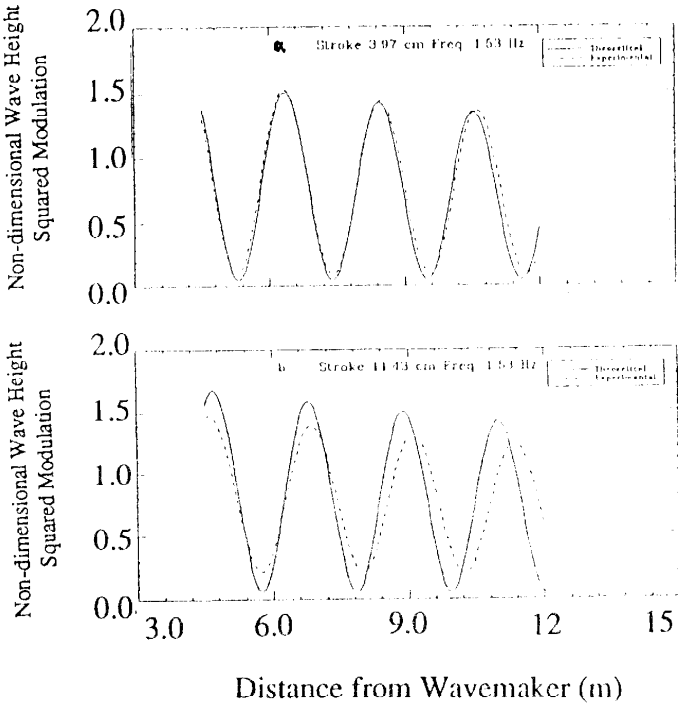

Figure 7. Local wave height modulation along the channel, with frequency of $f = 1.53$ Hz for wavemaker strokes of 3.97 cm and 11.3 cm.

corresponding wave slopes are very large; $\frac{H}{\lambda_0} = 0.257$ and $\frac{H}{\lambda_1} = 0.176$, where H is the total wave height measured 4.7 m from the wavemaker. These steepness ratios are much higher than the Stokes limiting steepness ratio of 0.17; it is, therefore, not surprising that breaking accompained these wave forms. Waves were breaking continuously throughout the length of the tank due to the nonlinear instability that arises from the steepness criteria. The nonlinear influence provide the impetus to closely examine the effect of a breaker on the underlying waves.

Figure 8 shows wave height-length relationships for short-crested waves as well as already existing criteria for two-dimensional waves. These measurements show that the criteria for breaking waves depend upon the short-crestedness of the waves and they are much smaller than the widely used Stokes criteria. The non-dimensionalized wave amplitude variation, $\frac{a_b}{a}$ where a_b and a are wave height during and before breaking process, respectively, is plotted in Figure 9 as a function of normalized time $t^* = \frac{2\pi t}{T}$, for a wavemaker with a period of 0.70 second and amplitudes of 13.97 cm and 11.43 cm, where T is the wave period. Up to the first quarter of the wave period, no reduction in wave amplitudes was observed. The reduction began in the second quarter of the period and continued up to the first half of the period where breaker size reached its maximum. It is clear from Figure 9 that the reduction in wave heights, as was shown in Figure 7, are strictly due to the existence of breakers throughout the maximum crests of the short-crested waves.

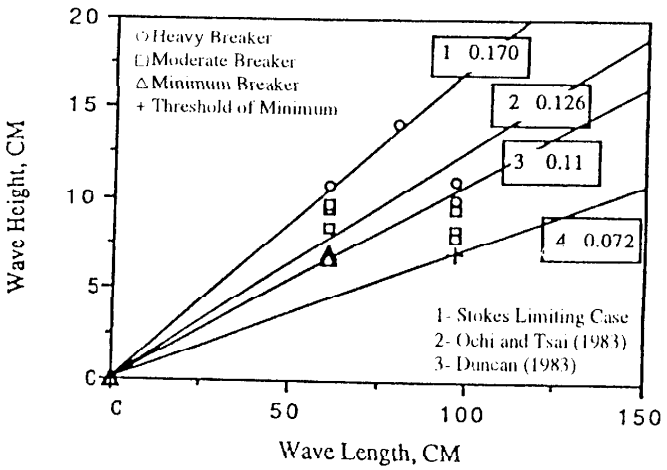

Figure 8. Criterion for breaking of steep, short-crested waves.

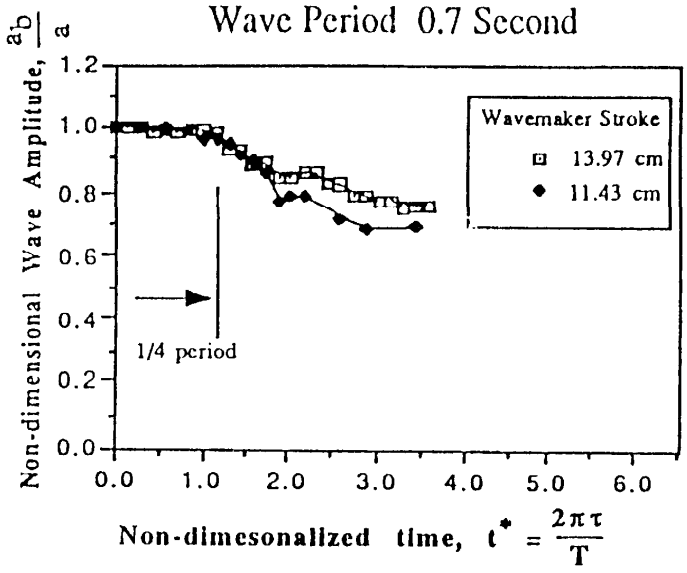

Figure 9. Dissipation of wave height due to breaker.

Figure 10 shows the generation of periodic solitons for frequency f = 1.299 Hz close to the first cut-off frequency. The non-dimensionalized soliton amplitude $|C(x,\tau)|$ is plotted against the normalized length, X, with advancing normalized time, τ [19]. This figure shows

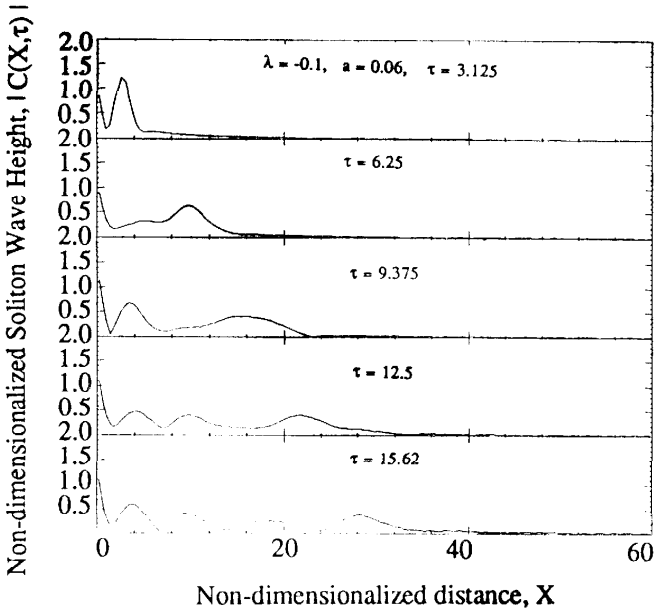

Figure 10. Numerical solution of modified nonlinear Schrodinger equation [19].

periodic generation of the soliton at the wavemaker with small modulation in the soliton height which is consistent with observed soliton height variation (Figure 5). The soliton speed was measured for several wavemaker forcing functions. For a given wavemaker stroke, the soliton's speed was measured to be constant. The soliton speed as a function of wavemaker stroke is shown in Figure 11. This figure shows a linear relationship between soliton speed and wavemaker stroke, with an off-set of approximately 2.7 cm which establishes the absence of a soliton at wavemaker strokes of less than 2.7 cm. There is no theroy available, so far, to predict these observations except the modified nonlinear Schrödinger where it qualitatively predicts the occurence of a propagation soliton.

CONCLUSIONS

The following conclusions are reached from this study:

1. The theoretical and experimental characteristics of the three-dimensional waves produced by plunging a half-cone wavemaker in a tank are given. This study may be useful for ocean wave simulation in experimental wave tank.

2. Even a monochromatic wave pattern exhibits considerable irregularity and complexity, which varies rapidly with changing frequency, especially upon passing cut-off frequencies, which are regularly spaced.

3. The linear theoretical prediction compares very well with the experimental measurements. At relatively moderate wavemaker stroke, these steep waves can be produced to break throughout a down channel of at least 15 tank widths. The reduction in wave heights between the predicted and measured ones are due to the existence of the breaker there. This effect was shown by experimental study of the breaking short-crested waves.

4. The criterion for steep short-crested waves is much smaller than those reported and it depends on the short-crestedness of the waves.

5. At a frequency close to the first cut-off frequency propagating, soliton waves were observed. The celerity of these solitons varies linearly with the wavemaker strokes and has an off-set of about 2.7 cm where existence of no soliton was observed. The modified nonlinear Schrödinger equation predicts the propagating of soliton waves and the numerical results show a qualitative agreement with the observed solitons but fails to predict the quantitative measurements.

6. The linear conical wavemaker theory can be modified to generate stochastic random waves in a laboratory narrow wave tanks, just like the ones at sea, for the purpose of studying random wave loads and breaking wave loads on the off-shore structures.

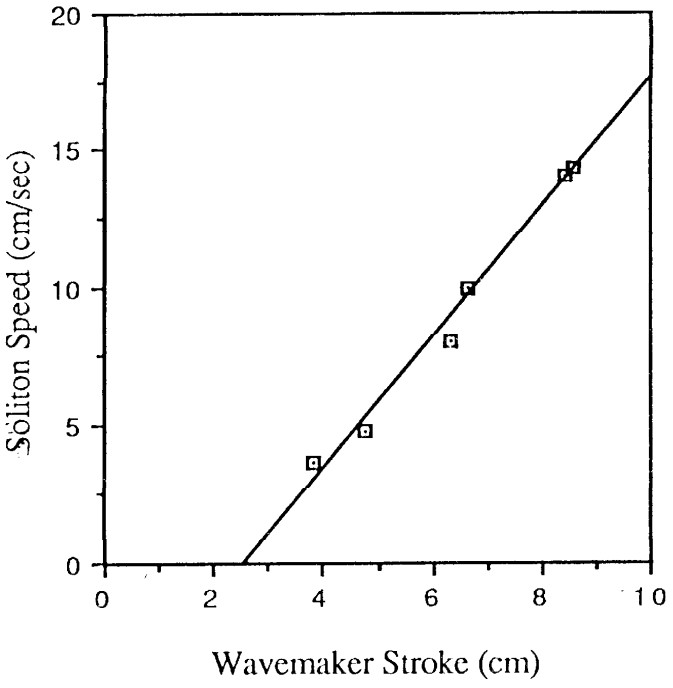

Figure 11. Soliton speed as a function of wavemaker stroke (experimental results).

ACKNOWLEDGEMENT

The author would like to thank M. P. Tulin for providing valuable suggestions and insights.

NOMENCLATURE

a	wave amplitude prior to breaking
a_b	wave amplitude after breaking

$a(y')$	source amplitude
$\tilde{a}(k)$	Fourier transform of $a(y')$
A_0	$\left(\frac{2}{\pi}\right)^{\frac{1}{2}}\left(\frac{R}{f}\right)\frac{(fk_0 + e^{-k_0 f} - 1)\, s}{fk_0}$, coefficient in Equation 11 for $n = 0$
A_1	$\left(\frac{k_0}{k_1}\right) A_0$, coefficient in Equation 11 for $n=1$
b	the tank width
$\|C(x,\tau)\|$	nondimensionalized soliton amplitude
f	cone height
g	gravity constant
h	tank depth
H	wave modulation height
k_0	$\frac{\omega^2}{g}$, wave numbeer
k_n	$\sqrt{k_0^2 - \kappa_n^2}$, wave number
K'	the attenuation coefficient
n	integer number
n_z	normal unit vector in z direction
n_r	normal unit vector in r direction
q(f)	source strength
r	$\sqrt{x^2 + y^2 + z^2}$
r'	$\sqrt{x^2 + (y - y')^2}$
r'_0	given in Equation. 6
R	cone base radius
s	wave maker stroke
t	time
x, y, z	cartesian coordinates
$\vec{V}$	(U, V, W), particle velocity vector
α	phase constant in Equation. 15
θ	$\sin^{-1}\left(\frac{1}{\omega^2}\right)$
ν	viscosity
$\zeta(x, y, t; \omega)$	free surface elevation
κ_n	$\frac{2\pi n}{b}$, wave number
λ_n	wavelength of the n^{th} mode
$\phi(x, y, t; \omega)$	potential function
ψ	phase function in Equation. 5
δ	cone angle

REFERENCES

1. T. H. Havelock, "Forced Surface Waves on Water," *Phil. Mag.*, Series 8(7), (1929), pp. 569-76.
2. O. S. Madsen, "Waves Generated by a Piston-type Wavemaker," *In Proceedings 12 Coastal Eng. Conf.*, Washington, D.C., Vol. 1, (1970), pp. 589-607.
3. O. S. Madsen, "On the Generation of Long Waves," *J. Geophys. Res.*, Vol. 36, (1971), pp. 8672-8683.
4. O. S. Madsen, "A Three-dimensional Wavemaker, Its Theory and Application," *J. Hydrraulic Res.*, Vol. 12, (1974), pp. 245-255.
5. S. Wang, "Plunger-type Wavemaker: Theory and Experiment," *J. Hydraulic Res.*, Vol. 12, (1974), pp. 357-387.
6. M. P. Tulin and A. R. Kolaini, " Steet Short-crested Waves Produced by a Simple Three-dimensional Wavemaker," *ATTC*, Washington D.C. (1986).
7. H. Lamb, "Hydrodynamics", Dover Publications, New York, (1932).
8. F. Ursell, "Edge Wave on a Sloping Beach," *Proceedings Roy. Soc. London*, A, Vol. 214, (1952), p 79.
9. B. J. S. Barnard and W. G. Pritchard, "Cross Waves," part 2, *J. Fluid Mech.*, Vol. 55, (1972), pp 245-286.
10. L. Shemer, E. Kit and T. Miloh, "Measurements of Two- and Three-dimensional Waves in a Channel, Including the Vicinity of Cut-off Frequencies," *Experimental Fluid Mechanics*, Vol. 5, (1987), p. 66.
11. L. Shemer and E. Kit, "Long-time Evolution and Regions of Existence of Parametrically Excited Non-linear Cross-waves in a Tank," *J. Fluid Mechanics*, Vol. 209, (1989), pp. 249-263.
12. E. Kit, L. Shemer and T. Miloh, "Nonlinear Sloshing Waves Near Second Cut-off Frequency," *J. Fluid Mech.*, Vol. 1981, (1987).
13. J. Wu, R. Keolian and I. Rudnick, (1984), "Observation of a Non-Propagating Hydrodynamics Soliton", *Phys. Rev. Lett.*, Vol. 52, (1984), pp. 1421-1424.
14. A. Larranza and S. Putterman, "Theory of Non-propagating Surface-wave Solitons," *J. Fluid Mech.*, Vol. 148,

(1984), pp. 443-449.

15. M. S. Longuet-Higgins, "The Unsolved Problem of Wave Breaking," *Proceedings, 17th Int. Conf. Coastal Eng.*, Sydney, Australia, (1980), pp. 1-28.
16. M. K. Ochi and C. H. Tsai, "Prediction of Occurrence of Breaking Waves in Deep Water," *J. Physical Oceanography*, Vol. 13, (1983), 2008-2019.
17. M. P. Tulin and R. Cointe, "Breaking Waves at Sea: Modelling and Applications," *Proceedings of the ASME-OMAE Houston Conference*, Houston, TX, (1988).
18. T. H. Havelock, "Waves Due to a Floating Sphere Making Periodic Heaving Oscillations," *Proceeding Roy. Soc.*, Series A, Vol. 231, (1955), pp. 1-7.
19. A. R. Kolaini, "Theoretical and Experimental Studies of Steep, Short-crested Waves Produced by a Conical Wavemaker," Ph.D. Dissertation, Dept. of Mechanical Engineering, UC Santa Barbara, (1989).
20. J. A. Aranha, D. K. P. Yue, and C. C. Mei, "Nonlinear Waves Near a Cut-off Frequency in an Acoustic Duct-a Numerical Study," *J. Fluid Mech.*, Vol. 121, (1982), pp. 465-485.
21. A-R. Kolaini and M. P. Tulin, "Experimental Studies of Unsteady Three-dimensional Spilling Breaking Waves," in the *Proceedings of the Third International Society of Offshore and Polar Engineering Conference* (ISOPE), Vol. 3, (1993), pp. 45-51.